Results from the ISSI Langmuir Probe Workshop: A 100-Year Workhorse, Easy to Fly but Difficult to Interpret

Laila Andersson*
University of Colorado Boulder, Boulder, CO, United States.

Takumi Abe†
Japan Aerospace Exploration Agency, Sagamihara, Kanagawa, 252-5210, Japan

Hassanali Akbari‡
NASA Goddard Space Flight Center, Greenbelt, MD, United States.

Edgar Bering§
University of Houston, Houston, Texas, 77204-5005, USA

John W. Bonnell¶
Space Sciences Laboratory, Univ. of Calif., Berkeley, CA, 94720-7450, USA

Anders Eriksson‖
Swedish Institute of Space Physics, Uppsala, SE-75137, Sweden

Jean-Pierre Lebreton**
LPC2E, Orleans and LESIA, Meudon , France

Wojciech Miloch††
University of Oslo, Oslo, Norway

Sylvain Ranvier‡‡
Royal Belgian Institute for Space Aeronomy (BIRA-IASB), Brussels, 1180, Belgium

One of the first instruments used to monitor laboratory plasmas was the Langmuir probe (LP). This instrument is still one of the key sensors in laboratory plasma investigations. With the access to space, the first sounding rockets with Langmuir Probes were flown in 1946-1947; followed with Langmuir probes on satellites from the early 1960s and on Pioneer Venus Orbiter and subsequent interplanetary probes starting in the 1970s. This paper summarizes some of the experiences of using Langmuir probes over the last 75-years in space, what issues have been encountered, and how to overcome different known effects unique to space flight measurements. This work was done through a number of workshops attended by a number of instrument team members and supported by the ISSI organisation.

I. Nomenclature

*Researcher, Laboratory of Space Physics
†Associate Professor, Japan Aerospace Exploration Agency, Sagamihara, Kanagawa, 252-5210, Japan
‡Research Scientist, Heliophysics Division, Bldg. 21, Rm 249
§Professor, Physics and ECE, PHYS 5005, Associate Fellow
¶Project Scientist, Space Science Laboratory, Univ. of Calif., Berkeley, CA, 94720-7450, USA.
‖Staff scientist, Swedish Institute of Space Physics, Uppsala
**Research Associate, LPC2E, Orléans, France
††Professor, Department of Physics, Postboks 1048 Blindern 0316
‡‡Researcher, Division of Space Physics

α_e = Contamination impact electrons coupling
α_i = Contamination impact impact coupling
β = Constant based on sensor shape
A_e = Collection area of the electrons
A_i = Collection area of the ions
C = Capacitance
dV/dV = Gradient in the IV-curve
dt_s = Bias sweep step time
dV_s = Bias sweep step in Voltage
FOV = Field-of-view
I_e = Electron current from the plasma to sensor
L = inductance
OML = orbital-motion-limited
R = resistance
SC = Spacecraft
SL = sheath limited
T_e = Electron temperature
u_{the} = Electron thermal speed
u_{thi} = Ion thermal speed
u_{SC} = Spacecraft speed
u_{the} = Electron thermal speed
u_{thi} = Ion thermal speed
V_s = Bias sweep potential
V_P = Plasma Potential
V_{SC} = Spacecraft potential

II. Introduction

Measurement of bulk plasma density and temperature is critical for our understanding of the space environment. As an example, the electron density and temperature drives many reaction rates in the thermosphere and ionosphere regions. Therefore, electron density (N_e) and temperature (T_e) measurements are important for any attempt to model or to predict the dynamics in these regions. Often the only *in situ* instruments that can provide this information are Langmuir Probes (LP). However, interpreting the measurements from a LP requires a scientific understanding of how the local plasma environment interacts with the probe and the spacecraft (SC). With more and more LPs flying, there is a need to have a common scientific understanding of how these interactions impact the measurements. The knowledge of how to interpret LP measurements in space has been presented in many papers. However, these papers are often individually incomplete, scattered across multiple journals over many decades, and often very focused on one particular spacecraft in one particular environment and one particular LP sensor design and its accommodation. Given the broad current interest in LPs, we empanelled a workshop team at the International Space Science Institute (ISSI) to capture and consolidate a century of hard-won knowledge and write down working knowledge that is seldom included in journal publications. In this paper, we present an overview of the efforts of the ISSI LP Workshop team, including the team's particular interest in such topics as: How to select LP sensor shape and accommodation? How do plasma flows around a spacecraft/sensor modify the current collected by the LP? Can LP measurements provide an accurate measurement of the spacecraft floating potential? How fast can the spacecraft/probe reach equilibrium with the surrounding plasma, and thus how rapidly can the plasma density and temperature be measured? What are the effects of magnetic fields on LP measurements? What limits the lowest and highest plasma temperatures measured by a LP? These topics are critical for interpreting the current and future generation of LP measurements. Our team composition was selected to provide experience from many different research teams that builds different high quality LP instruments.

A key aspect of LP data analysis resides in the interpretation of the Current-Voltage (IV) curves the LP produces. A LP instrument operates by varying the voltage bias applied on the sensor surface with respect to the spacecraft electrical ground and measuring the resulting the current collected by the sensor. The primary interest lies in the current arising from ambient electrons and positive ions. However, any other charge carriers near the LP (e.g. LP and SC photoelectrons and secondary electrons) contribute to the measured current, and their contributions may modify or even obscure the signal from the ambient plasma particles. Any physical obstructions to the field-of-view (FOV) of the LP,

electrostatic or magnetic barriers, or inhomogeneities of the LP collection surface may also contribute significantly to the shape of the measured LP curve. The team's has evaluated jointly the effects that have to be considered when trying to retrieve a physical parameter such as T_e and N_e from a measured LP curve. The team's has also assessed various techniques used to retrieve these parameters either directly through numerical derivatives of the LP curve, or through best-fit non-linear parametric models of the full LP curve.

The LP curve also provides information about the plasma potential, that is, the floating potential of the host SC relative to the electric potential in the nearby and distant plasma. Accurately identify this is important for the interpretation of the LP curve, as well as the data from other instruments on the host SC. This particular information has impact on any other payload instrument and that it should not change during the measurement the team discuss describes such effects and shows how such parameters may be extracted directly or indirectly from the LP curves in a separate discussion.

The data collected by other instruments and techniques complement those made by a LP. Such instruments and their data may be available on a given mission, or may be considered as part of a new mission design to enhance the probability of measuring the plasma parameters accurately enough to ensure full mission success. The team gathered a concise list of such complementary instruments and techniques, and here presents how they can improve the accuracy of LP measurements, and what additional resources and mission constraints such supporting instruments may require.

III. A Brief History of Langmuir Probes in Space

Irving Langmuir and Katherine Blodgett pioneered our understanding of this type of plasma diagnostic probe in 1923-1924 [1]. Mott-Smith and Langmuir followed the pioneering paper with their seminal work on how the current collected by a voltage-biased probe in a tenuous plasma depends on the electron density and temperature [2]. While these works were published well before the advent of the space age, modern researchers continue to use and reference these works, and a century after Langmuir's work, the Langmuir Probe (LP) is still the best instrument for measuring the core electron population characteristics of any plasma.

Sounding rocket flights of LP's began in 1946 with a series of three V2 flights from White Sands NMR in New Mexico, USA. Only the third flight in the series produced useful data [3]. Starting in 1958, a group of scientists at the University of Michigan began a series of sounding rocket flights intended to identify better choices of probe geometries [4]. The first flight tested an ejected subpayload design that was very innovative [4]. Since then, Langmuir probes on sounding rockets have often been used as part of auroral and ionospheric studies [e.g. 5–10].

Orbital use of LP's and closely related devices began with the launch of Sputnik 3. The Sputnik 3 SC carried an "ion trap", which was a boom mounted small sphere surrounded by a grid. The sphere was biased negative and the grid was swept. This device could measure ion density and infer spacecraft potential [11]. The first US orbital Langmuir probes were installed on Explorer VIII, which was launched in November, 1960 [12]. Explorer VIII was battery powered and had a very short mission. Fourteen days of useful LP data were obtained. The mission included 4 ion traps, 2 different Langmuir probes and an RF impedance probe. This mission was the first mission that allowed removal of the ion and photoemission currents, thus allowing the electron temperature to be estimated. Since then, LPs have been a mainstay of *in situ* aeronomy missions such as Explorer 17 (Atmosphere Explorer(AE)-A) [13], Explorer 22 [14]. Explorer 31 (AE-B) [15], Explorer 51 (AE-C), Explorer 54 (AE-D), Explorer 55 (AE-E) [16], Alouette II [15], and Explorer 63 (Dynamics Explorer-2) [17]. More recent Earth missions with LPs include Akebono [18], Astrid-2 [19], THEMIS [20], DEMETER [21, 22], Polar [23], Freja [24, 25], Swarm [26], and PICASSO [27]. Some of these missions, such as Astrid-2, DEMETER, and PICASSO, are examples of the growing power of small satellites.

Moving outward from LEO, the first detection of the solar wind plasma was made by a gridded ion analyzer (aka Faraday cup) carried on Explorer X [28]. These observations were made on the initial ascending leg of a 45 R_E apogee orbit. The use of LP's to study the ionospheres of other planets began with Pioneer Venus Orbiter [29]. Since then, LP's have studied Mars (Viking Lander [30] , MAVEN [31]), Saturn (Cassini [32]), a comet (Rosetta [33]), and the Sun (Parker Solar Probe [34]).

IV. The Concept of a Langmuir Probe: the IV-curve

A plasma contains both negatively and positively charged particles. When the particles hit and are absorbed by an exposed, biased conductor, a current can be measured. The measured current depends on the density and temperature of each species of the plasma and the potential between the plasma and the sensor. By biasing the sensor to a significantly negative potential with respect to the SC only the positive ions are collected. Conversely, with sufficiently positive bias

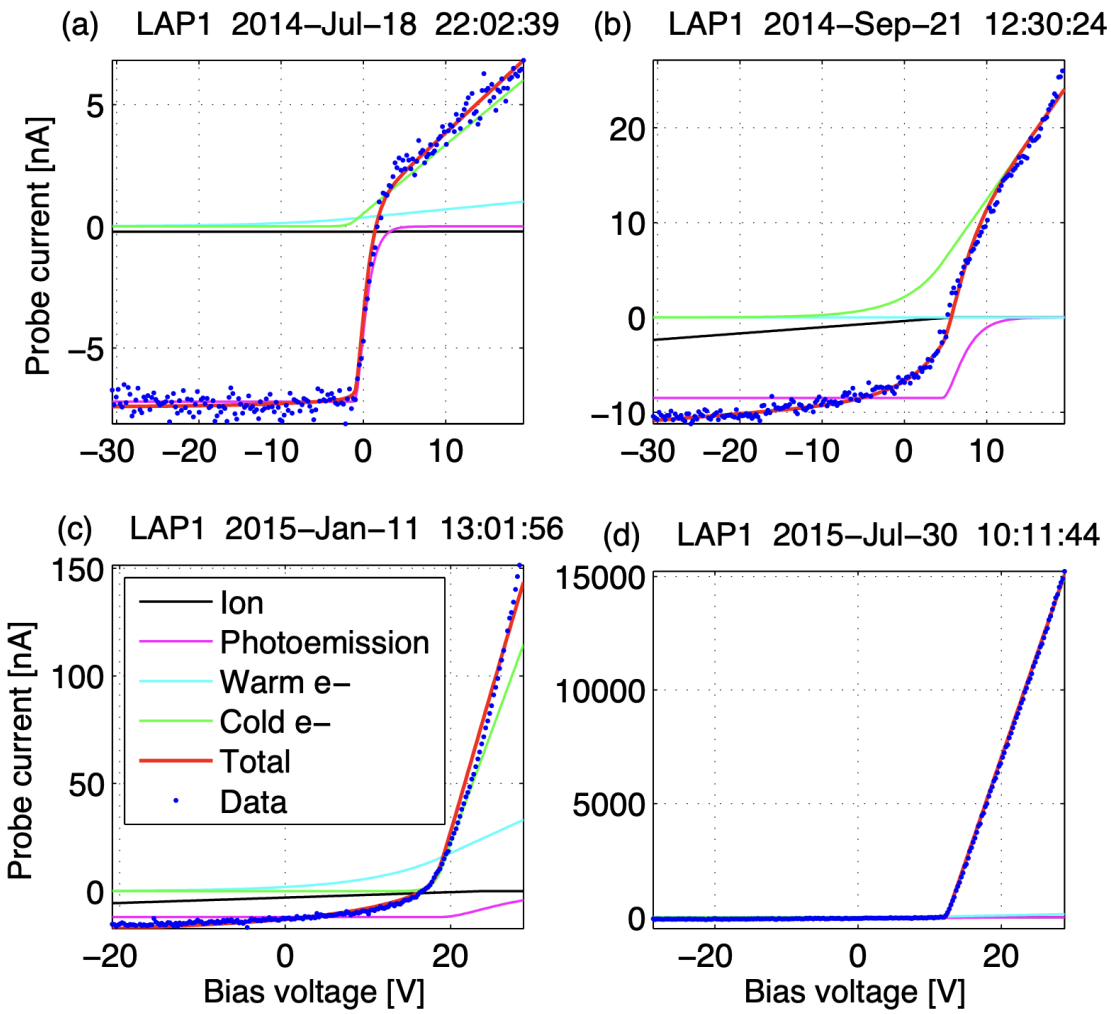

Fig. 1 Examples of Langmuir probe bias sweeps from one and the same instrument (LAP on Rosetta) in very different plasma environments. (a) Solar wind at 3.7 AU. In this tenuous plasma, the currents are only a few nA, dominated by probe photoemission (magenta) and collection of spacecraft photoelectrons (green). (b) Warm comet electrons (~10 eV, green) dominate the positive current in a low activity comet ionosphere. (c) Cold electrons mix in as comet activity increases. (d) Dense cold plasma near perihelion, with currents more than 3 orders of magnitude higher than in (a). Adapted from Eriksson et al. [33].

voltage only the negative particles are collected. For this paper the plasma is mostly assumed to only contain electrons and positive ions. By measuring the sensor current as function of applied bias voltage a current-voltage (IV) curve can be produced and examples of IV-curves measured in space during different plasma conditions are presented in Figure 1. From the IV-curve, plasma characteristics can be extracted either by comparison or fitting to some model of how the current depends on the parameters of the plasma or by the classical "graphical" method (Section IX). This idea is the fundamental principle of a LP. The LP is most sensitive to low energy particles and therefore primarily measures the bulk plasma, and is one of the few measurement techniques able to measure cold ($\lesssim$ 1 eV) plasma temperatures.

The standard convention, adhered to in this paper, is to count the probe current as positive when flowing from the probe to the plasma. The far negative side of the IV-curve is called ion saturation region, dominated by the current due to collection of plasma ions (I_i) and/or probe photoelectron emission (I_{ph}), while the far positive side is called electron saturation as it is dominated by the plasma electrons hitting the probe (I_e) and photoelectrons from the SC (I_{SC}). The main information that can be derived from these two regions usually are the electron and ion densities. The center part of the IV-curve ($I_i + I_e$) is the retarded region where the electron temperature and spacecraft potential (V_{SC}) are the key parameters to be extracted. The three regions are marked in Figure 2. Note here, plasma potential (V_P) and V_{SC} is often assumed to mean the same to make interpretations easier, but often they are not exactly the same.

V. The Different Currents Measured in Space

The prime currents of interest for LP measurements, that is the currents from the ambient plasma, are not the only currents that contribute to the measured current for space LP. These different currents need to be estimated and included in the data analysis to allow the plasma's density and temperature from the IV-curve to be extracted correctly. The total current to a Langmuir probe can be written as a sum of the various contributions:

$$I_{tot} = (1 - \alpha_e)I_e + (1 - \alpha_i)I_i + I_{ph} + I_{SC} + I_{dust} + I_{inst} \tag{1}$$

The plasma currents I_e and I_i depend mainly on the bias potential (V_s) and the spacecraft potential V_{SC}. The bracketed factors in front of I_e and I_i are included to account for possible effects of surface contamination, which we here use as an umbrella concept for many non-ideal surface effects (Section VI.C). The collected currents will also be impacted by instrument design, the location of the sensor on the SC with respect to the plasma flow velocity relative to the SC, and the plasma environment (Section VII). Even if the contribution of all different currents are understood the measured current might be decreased or increased over the expected theoretical value due to instrument design and mission implementation. We will use the term FOV to describe the geometric effects which modify the theoretical expected value. The FOV issues are the corrections that have to be done after the curve fitting based on theoretical assumptions are made. These corrections are usually done via empirical trends based on support measurements and will be discussed in Section IX. The paper will show that there are many different causes of FOV issues. How to compensate for different FOV issues is one of the key difficulties encountered while working with LP instruments.

Solar photons at energies above the work function of the sensor surface will cause photoelectron emission (I_{ph}) which contribute to the I_{tot}. Any other irradiated surface elements is the SC which also emit photoelectrons reaching the probe and contribute a current I_{SC} and contribute to the I_{tot} in a different fashion. That photoelectrons can impact the IV-curve in two different ways cna easily be overlooked. Both of these photoelectrons currents depend on solar irradiation (Irr), together with V_s and V_{SC}. The energy distribution of the photoelectrons is usually well described by a characteristic energy or temperature of a few eV [35–37].

Just as solar EUV photons, plasma particles with energies above the work function can cause secondary emission of electrons. Particularly for electrons of a few hundred eV energy, the secondary emission of electrons can lead to a significant current (I_{elec}) that can impact the net current (I_{tot}). The energy distribution of the secondary electrons can often be assumed to be similar to the photoelectrons.

For observations in dusty plasma such as meteoric layers in the ionosphere, dusty rings, plumes at moons etc the dust particles can themselves contribute to current, break apart, cause discharges or contaminate the probe. There is no general model for how dust will impact the I_{tot} and the reader is therefore advised to evaluate their specific conditions for how the dust impact their IV-curves.

Finally, every LP instrument may have leakage currents and offsets (I_{inst}). Much of this can be calibrated away on ground. However, with temperature variations and aging, these perturbations can evolve with time, and regular onboard calibrations are needed. Many instruments have included the hardware for this measurement into their design [20, 31, 38, 39]. Most of these instrumental effects are fairly uniform throughout the sweep and can be treated as a constant offset or a constant resistance when correcting for I_{inst}.

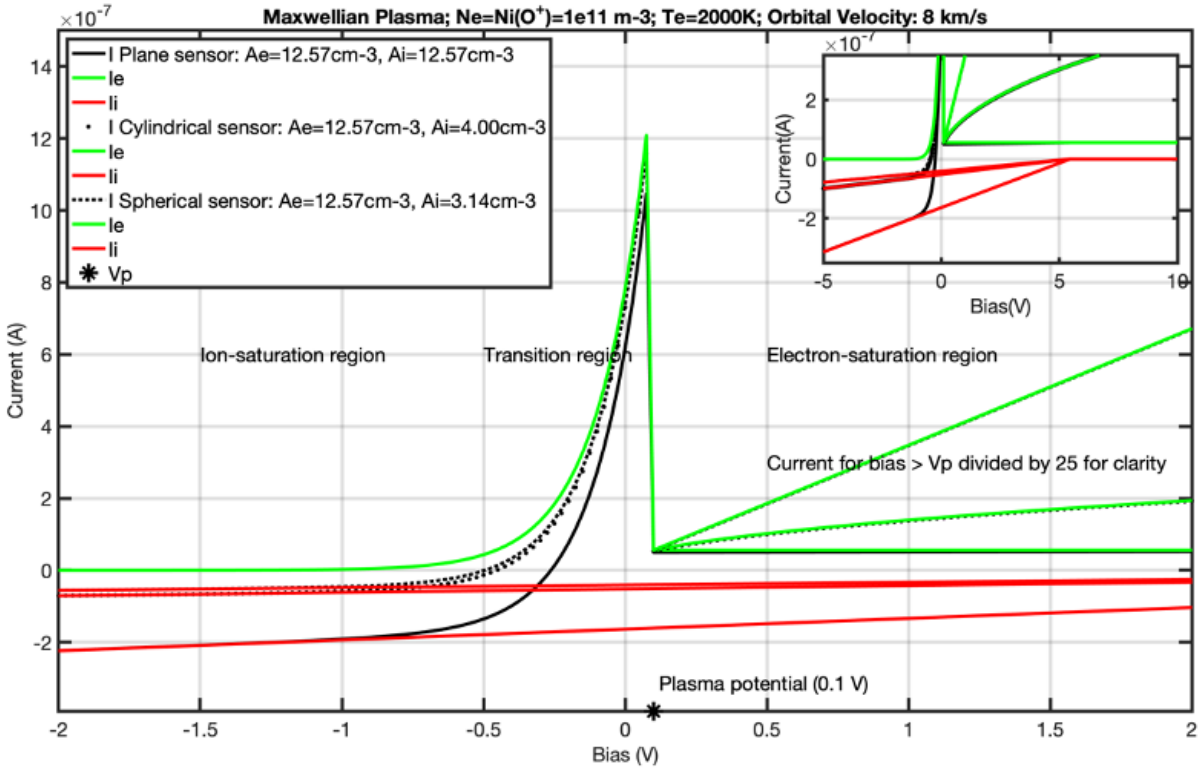

Fig. 2 Example of how ideal sensor shapes (Plane, Cylinder, Sphere) impact the the shape of the IV-curve (OML theory). The plasma parameters are indicated in the title of the figure. The plasma potential V_P has been arbitrarily chosen at 0.1 V. The electron collecting area of the sensor (A_e) is identical for all 3 geometries, while the collection area (A_i) of the ions ramming at orbital speed is different. Hence the collected electron current is identical for all 3 geometries up to the plasma potential (V_P). For increasing the visibility of the figure, the IV curve above the plasma potential V_P, is scaled by a factor of 25 for all 3 geometries. For $V > V_P$, the current is constant for a plane geometry, but varies as $(V - V_P)^{0.5}$ for a cylinder and $(V - V_P)^1$ for a sphere. That slope is usually refereed as the beta (β) factor.

VI. Different Plasma Environments

The plasma environments that LP instruments often are designed for require the instrument to operate over large temperature and density ranges. The target plasma together with the required accuracy of the measurement and limitations on the resources that can be used (cost, size, volume, and telemetry) all will drive the instrument design. In this Section the environmental drivers will be discussed.

A. Relative Motion between Sensor and Plasma

The primary impact of the relative speed of the SC and plasma is that it will drive the V_{SC}. The electron thermal speed is almost always much higher than SC speed ($u_{the} \gg U_{SC}$). For an electrically conducting SC surface, the total surface area is exposed to electron current, driving the SC toward negative potentials.

The ion thermal speed can be either larger or smaller that the SC speed ($u_{thi} > U_{SC}$ or $u_{thi} < U_{SC}$). In quasi neutral plasma and for small SC speeds the surface area is the same for electrons and ions, but as the electron thermal speed is usually much higher than the ion flow or thermal speed the resulting spacecraft potential V_{SC} is usually negative in dense plasmas where I_{ph} can be neglected. For $u_{the} > u_{SC} > u_{thi}$, which is the case for Low Earth orbit (LEO) the SC is ramming the ions so the area collecting ions is limited to the cross section area of the SC. For sounding rockets and LEO satellites, spacecraft potentials of -1 V to -3 V are common.

At high altitudes and low densities such as in the solar wind, the ion current is usually small in comparison to the electron and photoemission currents. As a result, spacecraft in such environments usually reach positive potentials. These potentials can vary from typically a few volts in the solar wind to tens of volts in very tenuous environments such as the Earth's geomagnetic tail or in a comet tail.

The relative speed of the probe to the plasma also influences how much of the surrounding plasma can reach the sensor. At subsonic flow speeds such effects are small. However, with supersonic flows around the sensor itself the collection of charges, particularly low energy electrons, that can reach the sensor can be modified by plasma structures developed by the plasma flowing around the probe and the spacecraft obstacles [40] and local plasma modification due to photoelectrons and magnetic fields. To first order, the ions are just ramming into the sensor (this was the example presented in Figure 2 resulting in the different collection areas) and behaves as the classical theory describes. However, there are three regions surrounding the sensor where the charge density is modified: an overdense region can form in front of the sensor due to the supersonic flow, an ion wake behind the sensor, and the flanks of the ion wake which also can be an overdense region stretching far from the sensor. The change in charge density results in modifications of the potential around the sensor resulting in the electron trajectories is altered and the electron current I_e to the probe start to deviate from classical theory. The phenomenon is the same as the wake behind and the overdense plasma in front of a SC observed by many missions [e.g. 19]. In high density regions the main impact usually is that wake edges guide electrons into the sensor creating a larger cross section than expected and I_e becomes larger than classical theory up to a factor of two [41]. The use of the collected I_e can therefore result in an overestimate of the density of the unperturbed plasma. This can be identified when compared to the ion current measured by the LP instrument or density measured from plasma waves instruments (Section X).

B. Small versus Large Debye Length

To derive plasma parameters from a Langmuir probe sweep, one needs some theoretical model of the probe response to the sweep potential. Useful such models can be derived for the ideal cases an infinite plane, and infinitely long cylinder, and an isolated sphere. While perfect realizations of these geometries are impossible, such models are useful in understanding real probes of planar, cylindrical and spherical shape, which means, therefore, that these models are in common use.

The probe current expressions will depend also on the fundamental plasma scale length, the Debye length λ_D. In a Langmuir probe context, its importance lies in that variations of charge density on scales shorter than λ_D will not create appreciable potentials. To first approximation, a probe (sphere or cylinder) of radius $r_p \ll \lambda_D$ therefore behaves as if in vacuum, with no appreciable shielding of its potential occurring in the probe sheath. Increasing the probe voltage then leads to higher current of the attracted particles. This case is known as the orbital motion limit (OML) case, for which well known theoretical relations apply [42, 43]. In the other extreme limit $r_p \gg \lambda_D$, the probe potential is shielded away completely in a distance small compared to the probe size. In this sheath limit (SL) or space charge limit case, increased probe voltage has little effect on the current. This is also the case for a planar probe of infinite extent, irrespective of λ_D. For the intermediate case of $r_p \sim \lambda_D$, even the idealized geometries are best handled by numerical simulations. Such simulations show that the OML results often hold well for Debye lengths down to probe radius, particularly for cylinders

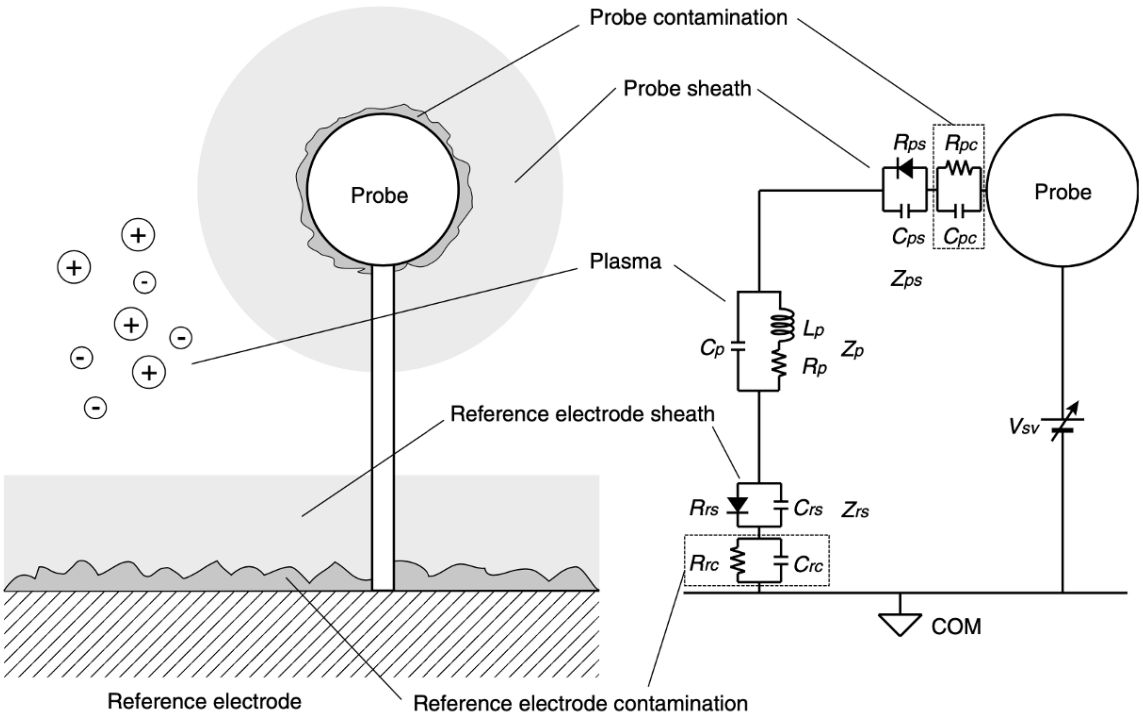

Fig. 3 Equivalent circuit of LP measurement. R, C and L represent resistance, capacitance and inductance, respectively. Subscripts pc, ps, p, rs and rc denote probe contamination, probe sheath, plasma, reference electrode sheath and reference electrode contamination. The diodes in the equivalent circuit represent non-linear resistance of the plasma sheath. Figure 1 from Shimoyama et al. [45]

[44].

A convenient way of quantifying the difference between the planar, cylindrical, and spherical shapes are by the β parameter and the theoretical curves is shown in Figure 2. In the theoretical description, the β parameter is 0 for an infinite plane, 1/2 for an infinite cylinder and 1 for an isolated sphere. For real probes, it is often found that the same expressions still apply well. However, the actual value of β will differ from these theoretical values as the planar sensor is often body mounted, the cylindrical probe is not infinitive long and the sphere is mounted on a boom. The relevant β value will also depend on the Debye length. At large λ_D cylindrical sensors will start to behave like a sphere while at sufficiently small λ_D all geometries will behave as (finite) planes ($beta \longrightarrow 0$). This resulting β value often lies between the theoretical values of the probe shape and will be changing with λ_D. If the environment that the LP instrument is flying in has a small dynamic range (e.g. λ_D is not varying much) then a fixed β value can be selected through in-orbit calibration. Otherwise, the β value needs to be presented as function of λ_D.

C. Probe Surface Issues

How a probe connects to the plasma and the SC is illustrated by Figure 3. An ideal Langmuir probe surface should be perfectly conductive. The additional physical and chemical requirements on a probe surface were discussed in detail by Brace [46]. The surface must have a uniform, stable work function. The surface must also be resistant to chemical changes caused by >5 eV atomic oxygen bombardment (most space applications have this issue), and as resistant as possible to adsorption of contaminants. The most important of these issues is work function uniformity. To illustrate the problem, let's consider this example. In the early 60's, electroplated rhodium was the probe coating of choice. When the spatial uniformity of the work function of electroplated rhodium was measured [47], it was found that the crystal domains formed macroscopic patches of uniform work function that differed from each other by $\leq$ 100 mV, owing to the fact that the Fermi surface of rhodium is not a sphere. Each of these patches will function as a separate probe with a different sweep voltage. The resulting sum of I-V curves flattens the slope, producing an over estimate of temperature.

This systematic error drives the requirement for probes to have as uniform a work function as possible. This requirement is met best by using a surface material with microscopic granularity. The main requirement is that any nonuniform in the surface micro (either area or potential) is small enough that it impact the mesoscale potential structure surrounding the sensor preventing the instrument to measuring the temperature the instrument is designed for. Any sensor surface issues will result in a warm temperature when extracting the information from the IV curve.

Even with the best selection of materials for the probe there are always potential issues with contamination, oxidation or other processes that complicate the coupling between the plasma and the sensor (Figure 3). Here we will use contamination as a umbrella word for all of these. Surface contamination can result in a charge layer acting as a capacitor in parallel with a resistor. Contamination effects can therefore often be modelled by adding a capacitance C and a resistance R between the probe and the plasma [48, 49]. If sweeping the probe voltage first in one direction and then in the other, the effect of an RC layer will then show up as an hysteresis effect. If the sweep is faster than RC time constant, the IV-sweep will be closer to an expected IV-curve while in case of contamination a slow sweep will be distorted compare to expected theoretical curve [50, 51]. However, depending on the probe to plasma time constant together with the spacecraft to plasma time constant, the sweep time might have to be slow to achieve the full sweep range. This later case can only be identified if a separate method is monitoring if V_{SC} is stable or changing during the sweep (such as an simple voltage probe).

As described before, this constant may be short compared to the sweep time steps the layer behaves as a resistor. In this case, α_e and α_i in Eq.(1) will be constant. In the other extreme limit of sweep stepping much faster than the RC time constant ($dt_s \ll RC$) the effect of the layer can be minimized and α_e, α_i goes to zero. Examples of the latter behavior can be found in Figure 5 of Lebreton et al. [52], where fast sweeps show much less hysteresis than slow sweeps.

Fast sweeps also minimize the effect of chemical changes in surface properties. At times, sensor surfaces can be dynamically modified by ion bombardment or chemisorbtion with CO, NO, N_2^+, or H [53–56]. Typically, these changes can be restored to original behaviours by floating the probe or by heating the sensor. What these dynamic chemistry issues imply is that both C and R may need to be treated as sweep-rate dependant. However, sweeping to fast require the instrument electronics can get to the right potential allowing a probe-spacecraft-plasma to be in a known equilibrium, e.g. just increase the sweep speed is not always the right solution.

VII. Examples of Different Instrument Designs

Langmuir probes for space applications need to be tailored to the mission under development based on the spacecraft, environment, and available resources. No design will work in every condition and all instrument designers must assess their needs for every application. Here the focus will be on the sensor mounting and how the potential around the SC impacts the shape of the IV-curve.

Physical and electrostatic blocking will in this paper be referred to as field-of-view (FOV) issues. And the mounting of the sensor needs to take this in consideration. Example, for a theoretical sensor with no SC present the contribution to the I_e current should be sum of the ram current and the wake current allowed by the potentials in the ion wake of the probe itself. However, the SC and structures extending from it can physically block the access of the electrons to the sensor. Furthermore, the SC and structures such as booms all extend their own electrostatic field into the surrounding space, interacting with the applied V_s on the sensor, impacting the motion of charged particles and therefore their possibility to reach the sensor. The potential structure will change with V_{SC}, so the impact on I_e is as function of both V_s and V_{SC}. In case of a spacecraft with significant areas at potentials deviating from the overall V_{SC} the situation becomes even more complicated.

A. Sensor Location and Size

The sensor location is critical to get the largest possible FOV for the instrument. As described above in Section VI.A, some of this concern is directly associated with λ_D and if ions are supersonic. In a supersonic flow, a location in the wake will obviously not be ideal for measurements of the unperturbed plasma. For a general purpose Langmuir probe, a good principle is to get several λ_D away from the large structures like the SC body. This principle usually means mounting the probe on some sort of boom, as slender as possible to minimize perturbations of the boom itself.

For special purposes, other mountings may still be useful. A planar probe mounted at the front of an ionospheric spacecraft can often provide good measurements of the density of O^+ and other heavy ions, whose ram energy of some 5 eV is well above the typical spacecraft potential (a few volts negative) so that their trajectories are not much influenced by the SC electrostatic field. However, such a probe could have severe issues with sampling electrons, whose possibilities to reach the probe may (depending on the detailed potential structure) be severely impacted by the

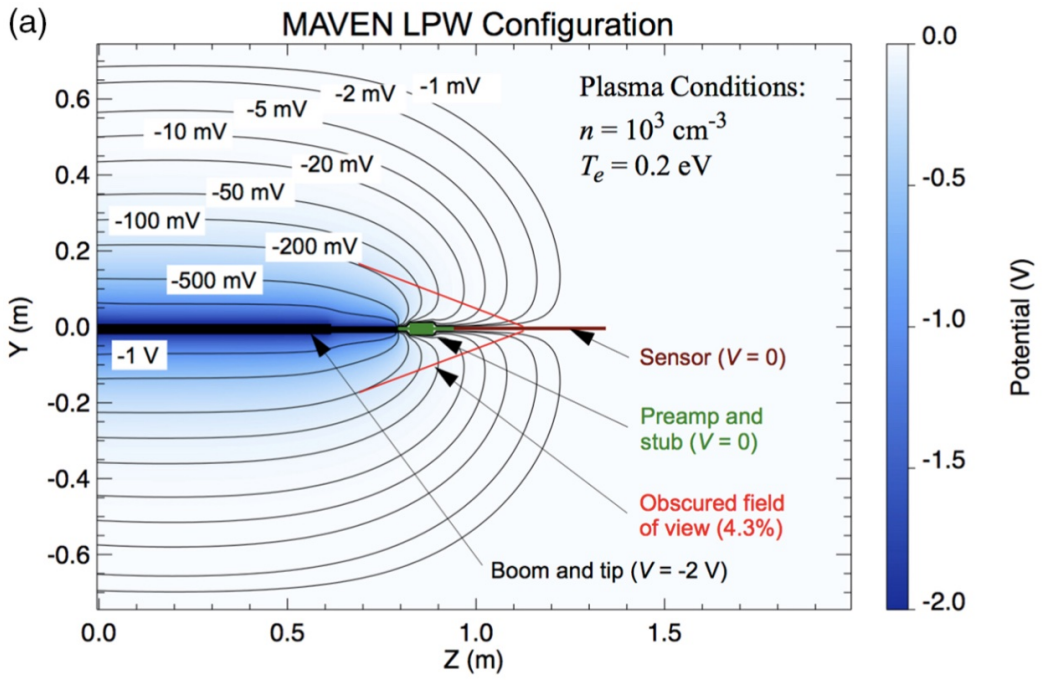

Fig. 4 Examples of potential barrier from the structure together with the sensor potential limiting the FOV. This potential structure changes with the instrument bias voltage sweep. Adapted from Ergun et al. [41].

spacecraft electrostatic field and might prevent any electron temperature to be estimated.

The selection of the location of the boom must change if potential noise sources (such as solar arrays) and structures that can modify the potential near to the sensor. Also, the attitude and possible spin of the SC need to be evaluated, including the expected directions of ram flow and solar illumination throughout the mission. As noted above, a normal requirement is to request the sensor to never be in the wake of the SC. To ensure stable illumination conditions another requirement could be to keep the sensor out of the shadow of the SC. Mounting two LP booms on opposite sides of the spacecraft usually result in these two requirements being met most of the time by at least one probe. While this approach might come with an extra cost, it can mean that LP instrument need not drive spacecraft pointing, simplifying operations planning and any later operation costs.

The LP instrument operates by pulling electron or ion current from the plasma. To maintain the probe-spacecraft-plasma to be in quasi neutrality, any current collected by the sensor from the plasma is expected to be closed through the SC body back to the plasma. The design requirement therefore needs to be that the SC is highly conducting and easily can close the circuit without changing its own potential. For conditions where $u_{the} > u_{SC} > u_{thi}$ when the sensor is attracting electrons, the SC body needs to attract ions. However, owing to the large difference in mobility, attracting enough ions can be difficult unless the surface area of the probe is small compared to the conductive cross section of the spacecraft. A good rule of thumb is the SC cross section should be at least 200 times larger [45, 57].

Not having a large conducting SC result in V_{SC} changes with respect to the plasma and the applied V_s is no longer with respect to a stable reference. A small reference surface (the RC-coupling between plasma ans sensor) also impacts the settling time for each sweep step and require a slow sweep time as discussed in Section VI.C. If the SC V_{SC} is not stable or monitored, the validity of the IV-curve decreases because V_{SC} will change during the sweep as function of V_s. On small spacecraft, the sensor-to-spacecraft surface ratio can be difficult to achieve. There are several different methods that have been proposed to compensate for this. Possible solutions to this problem include monitoring the spacecraft potential change with another probe [31, 39], use of so-called double probes for which the bias voltage is applied between two probes rather than between probe and spacecraft [e.g. 58, 59], sweeping very fast [45], or stabilizing the spacecraft potential by particle emitters [60].

B. Potentials Around the Sensor

Any structure of the SC or the boom holding the sensor will have a surface charge producing an electrostatic potential that superimposes on the potential from the sensor. With changing V_s, this interaction will change through out the sweep. If the sensor is not well placed and the surrounding potential well controlled there is a possibility that the potential structure from the sensor is shielded from the surrounding plasma. That is, a small change on V_s does not modify I_e significantly because the SC potential blocks the surrounding plasma from reaching the sensor. This blocking can be avoided with a well designed instrument.

Controlling the surfaces with known potentials around the sensor has several benefits. Stubs provide shadow or wake "equalization" to reduce the asymmetry introduced by the boom holding the sensor. Stubs also serve as DC electrostatic surfaces that make the potential distribution near the probe more uniform or closer to the free-space value (Figure 4).

Guards are biased surfaces along the booms between the inner stubs and the main SC body that provide low-energy electron current control (positive or negative potential barriers) to reduce stray currents from spacecraft or boom photoelectrons. To decrease currents such as photoelectrons from the spacecraft, a surface minimizing this current (a guard) is often biased built into the instrument design in such way that SC photoelectrons is deflected away from the sensor and the stub. The historical norm for this surface-bias design reached peak development on the Polar spacecraft [23].

To improve the FOV concerns and contribution of currents from other surfaces to the sensor the surfaces closest to the sensor is often biased in different ways depending on the design. Specially for cylinder sensor to mimic infinitely long sensor a segment next to the sensor of similar shape (a stub) is often held to the same potential as the sensor, i.e. sweeping with the LP sweep. This way the potential of the sensor expands and the FOV becomes improved. Additionally, modeling how the potential around the sensor as function of the instrument sweep need to be done to fully understand the response of the instrument.

C. Magnetic field effects

Magnetic field effects on Langmuir probes enter in several ways [61–63]. For a particle species with a gyroradius well below the size of the probe (its radius, for a cylinder or a sphere), the theoretical expressions for current collection changes as only particles on field lines intersecting the probe can reach the probe [64]. Because of the typical probe sizes and particle gyroradii in most space plasmas, this issue rarely needs to be considered.

Another effect is a FOV issue. Photoelectrons from the spacecraft may or may not reach the probe depending on the direction of the magnetic field, unless the gyroradius is large compared to boom length and spacecraft size. The current I_{SC} then depends on whether or not the magnetic field intersects both the sensor and a sunlit surface of the SC. This effect may need to either be minimized by sensor location or taken into account in the data processing. For the later case, the magnetic field vector in spacecraft coordinates must be known from either an onboard magnetometer or a good model.

A third effect concerns the $\vec{v}_{SC} \times \vec{B}$ electric field for a spacecraft moving through a magnetized plasma. A LP sensor is a conductor and hence the electric field along its surface is zero, in its own frame of reference – but not in the frame of the moving plasma. For a long cylindrical sensor shape, the potential difference between probe and plasma might vary significantly over its surface. Thus one end of the cylinder may attract electrons while the other end repels them, leading to a smearing out of the knee region from which electron temperature is estimated. The user has to assess if this is an issue for their application and instrument and either change the sensor shape, size or orientation, or accept that the instrument will not be able to measure the coldest temperatures. One should note that the effect also affects the spacecraft, so that even a perfectly conductive spacecraft will not be an equipotential from the point of view of the flowing plasma.

VIII. Instrument Operations

The instrument geometrical design and mounting location are not the only design factors to consider. Selecting a good way to operate the instrument will improve the understanding of the different factors impacting the IV-curve. On different space missions the telemetry, power usage, and the environment are all different resulting in different solutions. Here a few operation schemes are presented that may on may-not be prudent for other instruments.

A. Bias Voltage Sweeps

The step size in the voltage sweep (dV_s) determines how cold a plasma temperature can be measured from the IV-curve where dV_s needs to be smaller than the coldest temperature. Resolving the slope and hence the temperature requires several bias voltage steps within the transition region. The sweep range determines the range of (electron) temperatures that can be identified from the IV-curve and needs to be a few times wider than the warmest temperature of interest. Normally the telemetry and sweep frequency determine how many steps in the IV-curve will be measured by a specific instrument. Depending on instrument design the sweeps are pre-programmed in the instrument while more newer instruments have table look-up driven sweeps that can be updated on orbit.

The sweeps can be of many shapes: monotonic, up-and-down, a monotonic main sweep where in between each measurement the sensor is put to ground every time, sweeps that includes a jump from negative to positive then after a stable time jump back, to just to name a few. With table-driven sweeps, one may in principle apply the various voltages in a desired IV curve in any random order, not confining to a classical monotonic sweep. The sharp jumps, the ground potential between every sweep potential and up-and-down sweep all are designed to minimize or assess hysteresis and contamination effects. For some missions, this approach might just be used during the commissioning phase while on other missions this approach needs to be though out the mission.

The step size of V_s in the electron and ion saturation regions can be large while in the retarded region the smallest steps need to be applied as described above to resolve small temperatures. The smallest step sizes should be where one expects the knee region where T_e is extracted, i.e. close to V_{SC}. Since the V_{SC} often changes with plasma environment it is often not efficient to design the potential sweep where the step size are symmetric around the SC ground. Recent instruments often track approximate V_{SC} to apply the higher V_s resolution in the right voltage range. As an example, the MAVEN LPW instrument uses the zero current crossing from a previous IV-sweep plus a fixed offset is used as a guess for next sweep [31].

An alternative to classical sweeps is to use a ripple technique, where a high frequency (typically at least hundreds of Hz) variation is added to the bias voltage. With this technique, one does not only obtain the current I at a given bias voltage but also the slope dI/dV of the IV curve at that bias. By measuring at twice the applied frequency, d^2I/dV^2 can also be found, from which T_e and indeed the electron energy distribution function can be obtained [65, 66]. Several sounding rockets have used this technique, but the by far largest LP based dataset obtained by it derives from the three Swarm satellites, with N_e, T_e and V_{SC} values at 0.5 s resolution spanning (at the time of writing) ten years [26, 67]. For the SWARM mission every data point, I and dI/dV are first measured in the ion and electron saturation regions, defined by some sufficiently large fixed negative and positive bias values. The two lines thus obtained intersect in the retarded region where T_e is best measured, so there a third measurement is done to measure the electron temperature. Full sweeps are transmitted every few minutes for comparison. Besides reducing telemetry compared to transmitting full sweeps the ripple technique has the advantage of being more or less immune to probe contamination issues (Section VI.C) if the ripple frequency can be selected to be well above reasonable RC time constant, at the cost of more onboard processing and less complete information compared to sweeps.

B. Bias Sweep Program

The cadence (with which we here mean the interval between the start time of two consecutive sweeps) of the instrument needs to be based on the science requirements on what spatial or temporal scales should be resolved, together with what the telemetry allocation allows. The more points in the sweep that is measured improvement in the quality of the plasma parameters increases as they are extracted from the IV-curve. However, the number of sweep steps need to be selected based on sweep times, resolution needs, and telemetry limitations. Once the maximum cadence and number of points in the IV-curve have been identified the question becomes how fast should the sweep should be.

If the instrument is well coupled to the plasma one may in principle use the full measurement cadence, with the time for each sweep dt_s set to the cadence divided by the number of sweep steps. The timing of bias settings and current sampling is usually such that at each step in the sweep, the current is measured just before the next voltage step, to give time for the voltage to stabilize and the current to settle. Sometimes two or more measurements are taken at each step to allow assessment of any time constants in the system. However, if contamination of the probe is a concern (and the other aspects covered in (Section VI.C)) this operation methodology may not be the best approach. When I_{tot} is influenced by insulating film or capacitor build up, it is best to switch rapidly from V_s to next V_s in order to minimize any charge or contamination build up. This method can reduce the time it takes to do a full sweep resulting the time of a full sweep is much shorter than the cadence of the measurements [32].

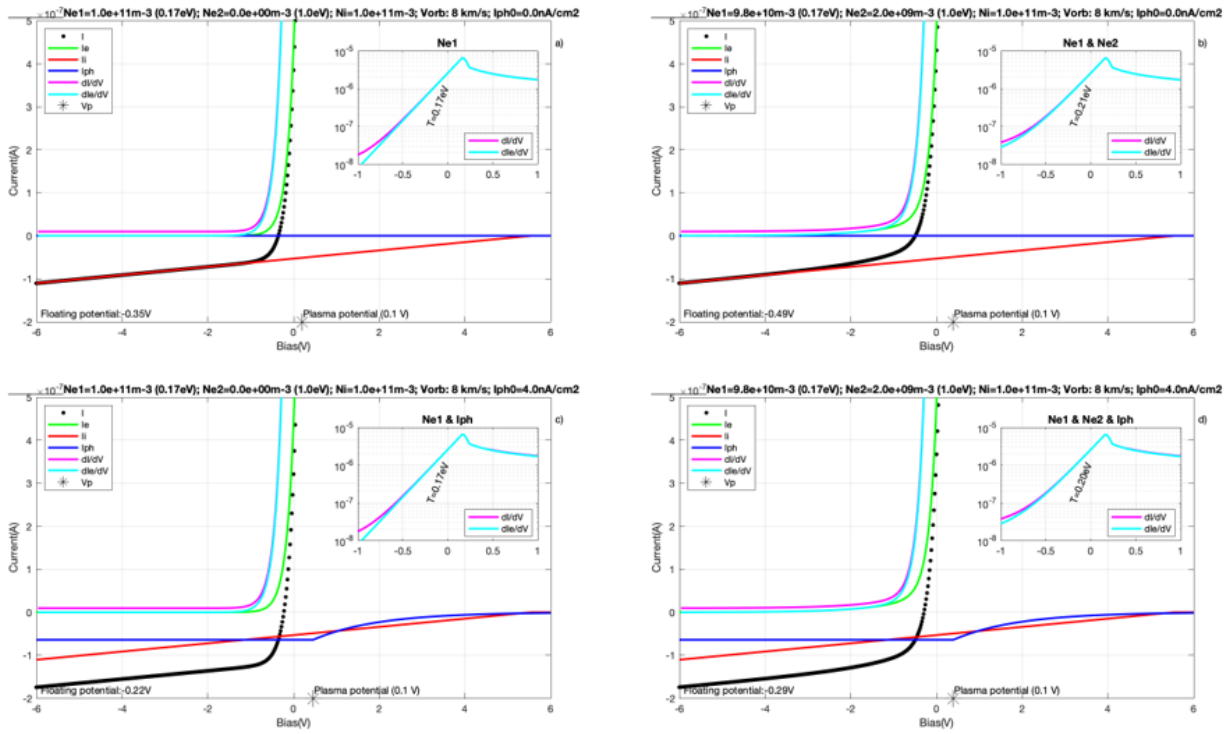

Fig. 5 Different combinations of contributing currents to the IV curve (Eq (1), using the OML formulae) for a cylindrical probe geometry are presented in four panels: panel a) one electron population, panel b) two electron populations, panel c) one electron population and photoelectrons, panel d) two electron populations and photoelectrons. In the main frame, IV curves are presented in linear scale as function of bias voltage V_s. In the inset, the numerical derivative of the total current I_{tot} and of the electron current I_e are shown. The photoelectron influences the determination of the probe floating potential, while it does not contribute to the derivative of the total current (I_{tot}) below Vp as it is constant. The two derivative curves overlap quite well around and below the plasma potential. Hence the plasma potential may be estimated from the maximum of either derivative. The plasma temperature is estimated from the slope (in semi-logarithmic scale) of the derivative of I_e, dIe/dV) in the transition region. When a (warmer) second electron population is present, the determined temperature using the method of the slope is higher.

IX. Interpreting Quantities From the IV-curve

When a IV-curve has been acquired in space several currents in Eq. (1) need to be subtracted (to isolate I_e and I_i) in order to extract the main parameters, N_e, T_e, and N_i. However, for most instruments, I_{inst} and I_{elec} result in a constant contribution through out the IV-curve and both can be treated as constant offsets and be identified by assuming a quasineutral plasma and comparing the electron and ion densities derived from the two saturation regions and requiring them to be equal. The I_{pho} depends on the EUV intensity, and it has a known temperature of a few eV [35–37]. The I_{pho} is constant for a bias below V_{SC} and decreases exponentially above V_{SC}. In contrast, the I_{SC} which is due to the same type of electron population as the phototoelectron current, but is emitted from the SC/boom, and it has the similar characteristics but contributes to the negative side of the sweep. How the I_{dust} contributes to the IV-curve if present depends on the mission details and therefore cannot be reviewed in a generic description.

To illustrate how the plasma parameters can be extracted a subset of the current contributing to Eq. (1) (often the dominant currents) is illustrated in Figure 5. Here I_e, I_i and I_{pho} are presented by a green, red, and blue curves respectively and I_{tot} by a black dotted line. Note that, since the different contributing currents have different signs, the I_{tot} is not always the line with the largest value. In Figure 5 theoretical IV-curves demonstrating the current contributions for a cylindrical probe geometry with: a) one electron population, b) two electron populations, c) one electron population and photoelectrons, d) two electron populations and photoelectrons. All curves are presented in a linear current scale as function of V_s. The derivative of I_{tot} and I_e are presented in an inset. The two methods to extract plasma parameters are detailed below.

Method 1: Referring to Eq. (1), under conditions that only I_i and I_e contribute significantly to the I_{tot}, it is possible fit the negatively-biased part of the IV curve, representing I_i, and to subtract it from the total current to isolate the I_e-V curve. T_e is obtained from the slope of the semilog plot of the retarding portion of the I_e-V curve [14, 21, 27, 45]. The plasma potential (V_p) may be obtained either at the location of the maximum of the numerical derivative of the I_e-V curve, or at the crossing of the polynomial fitting of the electron saturation current and the fitted curve to the slope of the electron retarding region. Under certain plasma conditions the derivative of the total current I_{tot} gives also a good approximation of the plasma potential. Ideally, assuming the OML theory applies, The fitting of the electron saturation portion of the I_e-V curve would be a flat line ($\beta = 0$) for a perfect (infinite) plane probe, a degree 2 parabola ($\beta = 1/2$) for perfect (infinitely long) cylinder or a strait line ($\beta = 1$) for a sphere. The electron density is obtained from determining I_e at V_p. In the case the photo- and the secondary electron currents can be neglected, the ion density can be obtained from the value of the fitting of the ion portion of the curve at V_p.

Method 2: This method is based on the fitting of the total current IV-curve, with modelling all the current contributions. This fit is complicated because it is a multi variable fit (T_e, N_e, N_i, V_{SC}, and eventually I_{ph}). Even with using $N_e = N_i$ the weighing of the IV-curve for the variable is not equal and all variables often cannot be solved in one step but most algorithms solve this in an iterative way, N_e, N_i followed by V_{SC} and T_e and then using the last values to try to optimise the next round [31–33].

In addition to the main two methods described above, one may mention attempts to use an approach that consists in creating a library of analytically or PIC-simulated IV-curves that encompass all expected Plasma conditions, N_e, T_e, V_{SC}. The model may also account for several physical effects of importance in the interaction of the probe sensor and the spacecraft with the space plasma environment. These include spacecraft charging, spacecraft wake, photoelectrons, and secondary electrons [22, 68–70].

It is worth noting that the accuracy of the derived plasma parameters is based on the sweep range of the sweep, the step size of the sweep, together with how accurately the current can be measured. The fitted quantities N_e, N_i, V_{SC} and T_e do not have errors with them, they are described by the best fitted value which comes with an uncertainty range of the quantities. This is important to remember, LP instruments do not provide measurement errors in the reported quantities, the parameters is extracted from fitting resulting in uncertainties, however, the IV-curve has measurement errors associated with it.

X. Supporting Measurements

As discussed in detail above, if one has an accurate estimate of the LP's FOV (effective collection area), its bias voltage relative to the local plasma, and the species and populations present in the plasma, then one can convert LP I-V sweeps into quite accurate relative density and electron temperature estimates. However, any uncertainties in those calibration parameters directly reduce the absolute accuracy of the density and temperature estimates but factors of at least 2 in practice, regardless of the stability and precise calibration of the basic LP instrument. A variety of additional plasma and field measurements can improve the accuracy of LP-based estimates of the local plasma density

and temperature by providing either absolute estimates of both quantities, or estimates of the parameters that affect the LP's FOV, or both.

First, one can measure the local vector magnetic field and plasma flow to estimate any finite electron gyroradius, magnetic wake, drift wake, and trans/supersonic effects on the LP's FOV. A DC magnetometer and either an ion drift meter or double probe electric field instrument provide the data required to see if the LP lies in the magnetic or drift wake of the SC or of its own boom, if the local electron gyroradius is on the order of the LP's dimensions, if the plasma flow lies in the sub-, trans-, or supersonic regime (the β value), or if there's a significant gradient in sheath voltage along the LP's surface. Modeling or analysis can determine a higher-accuracy FOV that enables higher-accuracy absolute calibration, or the times when these effects render the nominal FOV highly-inaccurate and the derived density and temperature suspect. In addition, the sensor-to-SC potentials measured by the E-field probes during LP IV sweeps will constrain the magnitude of SC floating potential variations, the uncertainty in the LP's bias voltage relative to the local plasma potential, and thus uncertainties in the LP electron temperature estimates.

Second, one can utilize double-probe electric plasma wave measurements near the local plasma or upper hybrid frequency to observe natural plasma instabilities (the "Langmuir line" technique) or quasi-thermal noise fluctuations (QTN technique) that provide absolute estimates of the local plasma density and electron temperature. When such measurements are available, past experience on auroral and solar wind missions [71–73] show that well-designed instruments utilizing accurate spectral fitting algorithms provide density estimates to better than 10%. Plasma frequency, impedance, or mutual impedance probes [74, for example] provide for similar absolute estimates of local plasma density, temperature, and collisionality with similar precision. Acquiring such data depends on a quiet electromagnetic environment (for QTN) or the presence of natural plasma instabilities (for Langmuir line), or both, and so may not be available for a given SC and plasma environment at all times or in all environments.

Third, one can utilize direct measurements of the electron and ion velocity distribution functions (VDFs) to constrain the actual value of the SC floating potential, to determine if returning SC photoelectrons are a significant flux in the environment, and determine the direct and secondary contributions of suprathermal and energetic electron and ion fluxes to the measured electron and ion currents at the LP. Integral VDF instruments such as ion drift meters, retarding potential probes, Faraday cups, and differential VDF instruments such as electrostatic and magnetic analysers all provide such supporting data as long as sufficient fluxes at high enough energies (typ. a few eV) are present. However, such measurements at these higher energies can not replace LP-based estimates of T_e in ionospheric plasmas, and if T_e is an important parameter, an LP instrument is almost all ways required.

Thus, if resources allow, hosting an LP as part of a suite of additional instruments increases its accuracy and utility. Careful and regular and in-flight inter-calibration of this suite of instruments allows for the best fusion of the full suite's data into the highest quality density and temperature estimates. A great example of this sort of in-flight calibration may be found in some of the earliest flights of LPs in the auroral ionosphere where thoughtful instrument design in terms of on-board current and voltage sources and flexible sensor biasing schemes allowed for the collection of a rich set of inter-calibration data that allwed for further more accurate interpretation of the measurements [58]. Such in-fight calibration activities may be combined with remote sensing techniques such as incoherent scatter radar (ISR) that provide a low-temporal and spatial resolution (seconds to tens of seconds; tens of km) estimate of electron temperature and density during planned or incidental conjunctions between the radar site and the orbiting SC.

XI. Conclusion

The Langmuir probe is a 100 year old workhorse that is one of the most used instrument for laboratory plasma experiments. It has been used in space to diagnose the plasma density and temperature since the first sub-orbital sounding rocket flights (1946-1947) and orbital satellites (1959 and onward). After decades, the LP remains a key element and mainstay of space plasma instrumentation - easy to build; consuming a modest amount of mass, power and telemetry; and one of the only instruments able to measure the thermal electron temperature in many plasma environments. However, interpreting the measured IV-curve requires significant care in understanding what is included in the measured current and how to interpret that current's variation with bias voltage in terms of the ambient plasma parameters. Above, we've summarized the relevant instrument and mission design parameters built up over the past 70-100 years to allow future LP instrumentalists and scientists to achieve the performance needed on a given mission, the accurate extraction of plasma parameters from the LP data itself, and the glorious new discoveries in ionospheric, planetary, and magnetospheric physics such data will enable.

Acknowledgments

The presented paper here is an extract of topics that was discussed and are worked into a larger work during a ISSI work group activity. ISSI facilitates workshops on many topics, selected through annual proposal rounds where an internationally diverse team can submit a workshop proposal on a specific area of scientific interest, such as the interpretation of LP data in space. Once selected the team works remotely and then in person at one of the ISSI locations where ISSI is the host. The selections are competitive covering a large span of scientific area such as astrophysics, heliophysics, and atmosphere.

Our team is contain members from some of the leading science groups from USA, Japan, Sweden, Norway, France, and Belgium. The team has experience with >20 sounding rockets, satellite missions, and interplanetary probes such as: Akebono, THEMIS, Demeter, MAVEN, Freja, Swarm, Polar, Rosetta, Parker Solar Probe, PICASSO, and many upcoming missions such as BepiColombo, GDC, JUICE, and Comet Interceptor. The team brings decades of experience in finding the different features that needs to be considered in order to interpret the measured LP IV-curve and to understand how different design choices affects the measurements. During the remote and in-person workshop activities, the team determined the salient features of LP across all prior and expected missions and environments, collected the relevant theoretical and observational references and data on those features, and synthesized this information into several published works.

This research was supported by the International Space Science Institute (ISSI) in Bern, through ISSI International Team project 488 (Langmuir Probes, a 100 Year Workhorse: Easy to Fly but Difficult to Interpret). The individual researchers have be supported by their founding agencies and projects. JWB acknowledges the support of the NASA Parker Solar Probe Fields contract and LIEFSI award at UCB for partial support of his work on this effort. LA acknowledges the support of the NASA mission contract for the MAVEN project in the Planetary division and the upcoming NASA GDC mission under the instrument AETHER contract under the Heliophysics division.

References

[1] Langmuir, I., and Blodgett, K. B., "Currents limited by space charge between coaxial cylinders," *Physical Review*, Vol. 22, No. 4, 1923, p. 347.

[2] Langmuir, I., and Mott-Smith, H., "The theory of collections in gas discharges," *Physical Review*, Vol. 28, 1926, p. 727.

[3] Hok, G., Spencer, N. W., and Dow, W. G., "Dynamic probe measurements in the ionosphere," *Journal of Geophysical Research (1896-1977)*, Vol. 58, No. 2, 1953, pp. 235–242. https://doi.org/https://doi.org/10.1029/JZ058i002p00235, URL https://agupubs.onlinelibrary.wiley.com/doi/abs/10.1029/JZ058i002p00235.

[4] Boggess, R., Brace, L., and Spencer, N., "Langmuir probe measurements in the ionosphere," *Journal of Geophysical Research*, Vol. 64, No. 10, 1959, pp. 1627–1630.

[5] Bering, E. A., and Mozer, F. S., "A Measurement of Perpendicular Current Density in an Aurora," *J. of Geophysical Research*, Vol. 80, No. 28, 1975, pp. 3961–3971.

[6] Abe, T., Oyama, K.-I., and Kadohata, A., "Electron temperature variation associated with the auroral energy input during the DELTA campaign," *Earth, planets and space*, Vol. 58, No. 9, 2006, pp. 1139–1146.

[7] Oyama, K.-I., Abe, T., Mori, H., and Liu, J., "Electron temperature in nighttime sporadic E layer at mid-latitude," *Annales Geophysicae*, Vol. 26, Copernicus GmbH, 2008, pp. 533–541.

[8] Di Mare, F., Spicher, A., Clausen, L. B. N., Miloch, W. J., and Moen, J. I., "Turbulence and intermittency in the winter cusp ionosphere studied with the ICI sounding rockets," *Journal of Geophysical Research: Space Physics*, Vol. 126, No. 8, 2021, p. e2021JA029150.

[9] Giono, G., Ivchenko, N., Sergienko, T., and Brändström, U., "Multi-Point Measurements of the Plasma Properties Inside an Aurora From the SPIDER Sounding Rocket," *Journal of Geophysical Research: Space Physics*, Vol. 126, No. 7, 2021, p. e2021JA029204.

[10] Pérez-Coll Jiménez, J., Ivchenko, N., Giono, G., Tolis, C., and Sergienko, T., "Analysis of multi-point Probe Measurements Obtained by SPIDER-2 Sounding Rocket in the Auroral E-region during a Pulsating Aurora Event," *AGU Fall Meeting Abstracts*, Vol. 2022, ????, pp. SA25B–1921.

[11] Krassovsky, V. I., "Exploration of the upper atmosphere with the help of the third Soviet sputnik," *Proc. IRE*, Vol. 47, 1959, p. 289.

[12] Serbu, G., Bourdeau, R., and Donley, J., "Electron temperature measurements on the Explorer VIII satellite," *Journal of Geophysical Research*, Vol. 66, No. 12, 1961, pp. 4313–4315.

[13] Brace, L., Spencer, N., and Dalgarno, A., "Detailed behaviour of the midlatitude ionosphere from the Explorer XVII satellite," *Planetary and Space Science*, Vol. 13, No. 7, 1965, pp. 647–666.

[14] Brace, L., and Reddy, B., "Early electrostatic probe results from Explorer 22," *Journal of Geophysical Research*, Vol. 70, No. 23, 1965, pp. 5783–5792.

[15] Findlay, J. A., and Brace, L., "Cylindrical electrostatic probes employed on Alouette II and Explorer XXXI satellites," *Proceedings of the IEEE*, Vol. 57, No. 6, 1969, pp. 1054–1056.

[16] Brace, L., Theis, R., and Dalgarno, A., "The cylindrical electrostatic probes for Atmosphere Explorer-C,-D, and-E," *Radio Science*, Vol. 8, No. 4, 1973, pp. 341–348.

[17] Burch, J., and Hoffman, R., "Introduction to the Dynamics Explorer mission," *23rd Aerospace Sciences Meeting*, 1985, p. 61.

[18] Abe, T., OYAMA, K.-i., AMEMIYA, H., WATANABE, S., OKUZAWA, T., and Schlegel, K., "Measurements of temperature and velocity distribution of thermal electrons by the Akebono (EXOS-D) satellite experimental setup and preliminary results," *Journal of geomagnetism and geoelectricity*, Vol. 42, No. 4, 1990, pp. 537–554.

[19] Ivchenko, N., Facciolo, L., Lindqvist, P.-A., Kekkonen, P., and Holback, B., "Disturbance of plasma environment in the vicinity of the Astrid-2 microsatellite," *Ann. Geophys.*, Vol. 19, 2001, pp. 655–666.

[20] Bonnell, J., Mozer, F., Delory, G., Hull, A., Ergun, R., Cully, C., Angelopoulos, V., and Harvey, P., "The electric field instrument (EFI) for THEMIS," *The THEMIS mission*, 2009, pp. 303–341.

[21] Lebreton, J.-P., Stverak, S., Travnicek, P., Maksimovic, M., Klinge, D., Merikallio, S., Lagoutte, D., Poirier, B., Blelly, P.-L., Kozacek, Z., and Salaquarda, M., "The ISL Langmuir probe experiment processing onboard DEMETER: Scientific objectives, description and first results," *Planetary and Space Science*, Vol. 54, 2006, pp. 472–486.

[22] Imtiaz, N., Marchand, R., and Lebreton, J., "Modeling of current characteristics of segmented Langmuir probe on DEMETER," *Physics of Plasmas*, Vol. 20, No. 5, 2013.

[23] Harvey, P., Mozer, F., Pankow, D., Wygant, J., Maynard, N., Singer, H., Sullivan, W., Anderson, P., Pfaff, R., and Aggson, T., "The electric field instrument on the Polar satellite," *Space Science Reviews*, Vol. 71, 1995, pp. 583–596.

[24] Holback, B., Jansson, S.-E., Åhlén, L., Lundgren, G., Lyngdal, L., Powell, S., and Meyer, A., "The Freja wave and plasma density experiment," *The Freja Mission*, 1995, pp. 173–188.

[25] Marklund, G., Blomberg, L., Lindqvist, P.-A., Fälthammar, C.-G., Haerendel, G., Mozer, F., Pedersen, A., and Tanskanen, P., "The double probe electric field experiment on Freja: Experiment description and first results," *The Freja Mission*, 1995, pp. 79–104.

[26] Knudsen, D. J., Burchill, J. K., Buchert, S. C., Eriksson, A. I., Gill, R., Wahlund, J. E., Öhlen, L., Smith, M., and Moffat, B., "Thermal ion imagers and Langmuir probes in the Swarm electric field instruments," *Journal of Geophysical Research (Space Physics)*, Vol. 122, No. 2, 2017, pp. 2655–2673. https://doi.org/10.1002/2016JA022571.

[27] Ranvier, S., and Lebreton, J.-P., "Laboratory measurements of the performances of the Sweeping Langmuir Probe instrument aboard the PICASSO CubeSat," *Geoscientific Instrumentation, Methods and Data Systems*, Vol. 12, 2023, pp. 1–13. https://doi.org/10.5194/gi-12-1-2023.

[28] Bridge, H., Dilworth, C., Lazarus, A., Lyon, E., Rossi, B., and Scherb, F., "Direct observations of the interplanetary plasma," *Journal of the Physical Society of Japan, Vol. 17, Supplement A-II, Proceedings of the International Conference on Cosmic Rays and the Earth Storm, held 5-15 September, 1961 in Kyoto. Volume II: Joint Sessions. Published by the Physical Society of Japan, 1962., p. 553*, Vol. 17, 1962, p. 553.

[29] Krehbiel, J., Brace, L., Theis, R., Cutler, J., Pinkus, W., and Kaplan, R., "Pioneer Venus orbiter electron temperature probe," *IEEE Transactions on Geoscience and Remote Sensing*, , No. 1, 1980, pp. 49–54.

[30] Hanson, W., and Mantas, G., "Viking electron temperature measurements: Evidence for a magnetic field in the Martian ionosphere," *Journal of Geophysical Research: Space Physics*, Vol. 93, No. A7, 1988, pp. 7538–7544.

[31] Andersson, L., Ergun, R., Delory, G., Eriksson, A., Westfall, J., Reed, H., McCauly, J., Summers, D., and Meyers, D., "The Langmuir probe and waves (LPW) instrument for MAVEN," *Space Science Reviews*, Vol. 195, 2015, pp. 173–198.

[32] Wahlund, J.-E., Bostrom, R., Gustafsson, G., Gurnett, D., Kurth, W., Pedersen, A., Averkamp, T., Hospodarsky, G., Persoon, A., and Canu, P., "Cassini measurements of cold plasma in the ionosphere of Titan," *Science*, Vol. 308, No. 5724, 2005, pp. 986–989.

[33] Eriksson, A. I., Engelhardt, I. A. D., André, M., Boström, R., Edberg, N. J. T., Johansson, F. L., Odelstad, E., Vigren, E., Wahlund, J.-E., Henri, P., Lebreton, J.-P., Miloch, W. J., Paulsson, J. J. P., Simon Wedlund, C., Yang, L., Karlsson, T., Jarvinen, R., Broiles, T., Mandt, K., Carr, C. M., Galand, M., Nilsson, H., and Norberg, C., "Cold and warm electrons at comet 67P/Churyumov-Gerasimenko," *Astronomy and Astrophysics*, Vol. 605, 2017, p. A15. https://doi.org/10.1051/0004-6361/201630159, URL https://doi.org/10.1051/0004-6361/201630159.

[34] Mozer, F., Agapitov, O., Bale, S., Bonnell, J., Bowen, T., and Vasko, I., "DC and low-frequency electric field measurements on the Parker Solar Probe," *Journal of Geophysical Research: Space Physics*, Vol. 125, No. 9, 2020, p. e2020JA027980.

[35] Hinteregger, H. E., "Combined retarding potential analyses of photoelectons and environmental charged particles up to 232 km," *1st International Space Science Symposium*, North Holland Publishing Co., 1960.

[36] Pedersen, A., Fahleson, U., and Faelthammar, C., "Determination of ionospheric density and temperature using a double probe electric field detector," Report, Kungliga Tekniska Hoegskolan, 1971.

[37] Grard, R. J. L., "Properties of satellite photoelectron sheath derived from photoemission laboratory studies," *J. Geophys. Res.*, Vol. 78, 1973, pp. 2885–2906.

[38] Wygant, J., Bonnell, J., Goetz, K., Ergun, R., Mozer, F., Bale, S., Ludlam, M., Turin, P., Harvey, P., and Hochmann, R., "The electric field and waves instruments on the radiation belt storm probes mission," *The Van Allen Probes Mission*, 2014, pp. 183–220.

[39] Ranvier, S., Anciaux, M., De Keyser, J., Pieroux, D., Baker, N., and Lebreton, J.-P., "SLP: The Sweeping Langmuir Probe Instrument to Monitor the Upper Ionosphere on Board the PICASSO Nano-Satellite," *Proc. 70th International Astronautical Congress (IAC)*, 2019, p. Paper ID 53780. URL https://orfeo.belnet.be/handle/internal/7529.

[40] Bering, E. A., "Properties of the wake of small Langmuir probes and sounding rockets," *Journal of Atmospheric and Terrestrial Physics*, Vol. 37, 1975, pp. 119–129.

[41] Ergun, R. E., Andersson, L. A., Fowler, C. M., and Thaller, S. A., "Kinetic Modeling of Langmuir Probes in Space and Application to the MAVEN Langmuir Probe and Waves Instrument," *Journal of Geophysical Research: Space Physics*, Vol. 126, No. 3, 2021, p. e2020JA028956. https://doi.org/https://doi.org/10.1029/2020JA028956, URL https://agupubs.onlinelibrary.wiley.com/doi/abs/10.1029/2020JA028956, e2020JA028956 2020JA028956.

[42] Mott-Smith, H. M., and Langmuir, I., "The theory of collectors in gaseous discharges," *Phys. Rev.*, Vol. 28, 1926, pp. 727–763.

[43] Laframboise, J. G., and Parker, L. W., "Probe design for orbit-limited current collection," *Physics of Fluids*, Vol. 16, No. 5, 1973, pp. 629–636. https://doi.org/10.1063/1.1694398, URL http://link.aip.org/link/?PFL/16/629/1.

[44] Laframboise, J. G., "Theory of spherical and cylindrical Langmuir probes in a collisionless, Maxwellian plasma at rest," Tech. Rep. UTIAS report 100, Institute for Aerospace Studies, University of Toronto, 1966.

[45] Shimoyama, M., Oyama, K., Abe, T., and Yau, A., "Effect of finite electrode area ratio on high-frequency Langmuir probe measurements," *Journal of Physics D: Applied Physics*, Vol. 45, No. 7, 2012, p. 075205.

[46] Brace, L. H., *Langmuir probe measurements in the ionosphere*, 1998, Vol. 102, pp. 23–35.

[47] Kelley, M. C., "Auroral zone electric field measurements on sounding rockets," Thesis, 1971.

[48] Oyama, K. I., "A systematic investigation of several phenomena associated with contaminated Langmuir probes," *Planetary and Space Science*, Vol. 24, 1976, pp. 183–190.

[49] Piel, A., Hirt, M., and Steigies, C. T., "Plasma diagnostics with Langmuir probes in the equatorial ionosphere: I. The influence of surface contamination," *Journal of Physics D Applied Physics*, Vol. 34, 2001, pp. 2643–2649. https://doi.org/10.1088/0022-3727/34/17/311.

[50] Szuszczewicz, E. P., and Holmes, J. C., "Surface contamination of active electrodes in plasmas; Distortion of conventional Langmuir probe measurements," *Journal of Applied Physics*, Vol. 46, 1975, p. 5134.

[51] Szuszczewicz, E., and Holmes, J., "Observations of electron temperature gradients in mid-latitude Es layers," *Journal of Geophysical Research*, Vol. 82, No. 32, 1977, pp. 5073–5080.

[52] Lebreton, J.-P., Stverak, S., Travnicek, P., Maksimovic, M., Klinge, D., Merikallio, S., Lagoutte, D., Poirier, B., Blelly, P.-L., Kozacek, Z., et al., "The ISL Langmuir probe experiment processing onboard DEMETER: Scientific objectives, description and first results," *Planetary and Space Science*, Vol. 54, No. 5, 2006, pp. 472–486.

[53] Fukuda, Y., Lancaster, G., Honda, F., and Rabalais, J., "Chemisorption of CO on (1011) titanium studied by XPS, UPS, FDMS, and AIB," *The Journal of Chemical Physics*, Vol. 69, No. 8, 1978, pp. 3447–3452.

[54] Lancaster, G. M., and Rabalais, J. W., "Chemical reactions of N2+ ion beams with first-row transition metals," *Journal of Physical Chemistry*, Vol. 83, No. 2, 1979, pp. 209–212.

[55] Rabalais, J. W., and CHEMISTRY, H. U. T. D. O., "Interactions of Molecular and Ion Beams With Surfaces," *Final Report*, 1979.

[56] Fukuda, Y., Honda, F., and Rabalais, J. W., "Chemisorption of NO and NH3 on rhenium studied by UPS, XPS, TDS and work function measurements," *Surface Science*, Vol. 99, No. 2, 1980, pp. 289–299.

[57] Hershkowitz, N., *How Langmuir probes work*, Academic Press, Inc., San Diego, 1989, pp. 114–181.

[58] Fahleson, U., Fälthammar, C.-G., and Pedersen, A., "Ionospheric temperature and density measurements by means of spherical double probes," *Planet. Space Sci.*, Vol. 22, 1974, pp. 41–66.

[59] Stenzel, R. L., "A new probe for measuring small electric fields in plasmas," *Review of Scientific Instruments*, Vol. 62, 1991, pp. 130–139. https://doi.org/10.1063/1.1142514, URL https://ui.adsabs.harvard.edu/abs/1991RScI...62..130S.

[60] Bekkeng, T. A., Helgeby, E. S., Pedersen, A., Trondsen, E., Lindem, T., and Moen, J. I., "Multi-Needle Langmuir Probe System for Electron Density Measurements and Active Spacecraft Potential Control on CubeSats," *IEEE Transactions on Aerospace Electronic Systems*, Vol. 55, No. 6, 2019, pp. 2951–2964. https://doi.org/10.1109/TAES.2019.2900132.

[61] Sanmartin, J. R., "Theory of a probe in a strong magnetic field," *The Physics of Fluids*, Vol. 13, No. 1, 1970, pp. 103–116.

[62] Schmitt, J., "Wake past an obstacle in a magnetized plasma flow," *Plasma Physics*, Vol. 15, No. 7, 1973, p. 677.

[63] Darian, D., Marholm, S., Paulsson, J. J. P., Miyake, Y., Usui, H., Mortensen, M., and Miloch, W. J., "Numerical simulations of a sounding rocket in ionospheric plasma: Effects of magnetic field on the wake formation and rocket potential," *Journal of Geophysical Research: Space Physics*, Vol. 122, No. 9, 2017, pp. 9603–9621.

[64] Sonmor, L. J., and Laframboise, J. G., "Exact current to a spherical electrode in a collisionless, large-Debye-length magnetoplasma," *Phys. Fluids B*, Vol. 3, 1991, pp. 2472–2490.

[65] Oyama, K. I., Hirao, K., Banks, P. M., and Williamson, P. R., "Nonthermal components of low energy electrons in the ionospheric E and F region," *Journal of Geomagnetism and Geoelectricity*, Vol. 35, No. 6, 1983, pp. 185–200. https://doi.org/10.5636/jgg.35.185.

[66] Raitt, W. J., and Thompson, D. C., "Thermal Plasma Measurements in Space Using Direct Measurements of Derivatives of Probe Current-Voltage Characteristics," *Geophysical Monograph Series*, Vol. 102, 1998, p. 43. https://doi.org/10.1029/GM102p0043, URL https://ui.adsabs.harvard.edu/abs/1998GMS...102...43R.

[67] Buchert, S., "Release notes for an extended set of Swarm Langmuir probe data," Tech. Rep. SW-RN-IRF-GS-005, Swedish Institute of Space Physics, 2016. URL https://swarm-diss.eo.esa.int/?do=download&file=swarm/Advanced/Plasma_Data/2_Hz_Langmuir_Probe_Extended_Dataset/SW-RN-IRF-GS-005_Extended_LP_Data_Probes.pdf.

[68] Olowookere, A., and Marchand, R., "A New Technique to Infer Plasma Density, Flow Velocity, and Satellite Potential From Ion Currents Collected by a Segmented Langmuir Probe," *IEEE Transactions on Plasma Science*, Vol. 50, No. 10, 2022, pp. 3774–3786.

[69] Imtiaz, N., and Marchand, R., "Particle-in-cell modeling of Dual Segmented Langmuir Probe on PROBA2," *Astrophysics and Space Science*, Vol. 360, 2015, pp. 1–8.

[70] Marchand, R., Shahsavani, S., and Sanchez-Arriaga, G., "Beyond analytic approximations with machine learning inference of plasma parameters and confidence intervals," *Journal of Plasma Physics*, Vol. 89, No. 1, 2023, p. 905890111. https://doi.org/10.1017/S0022377823000041.

[71] Moore, T. E., Pollock, C. J., Adrian, M. L., Kintner, P. M., Arnoldy, R. L., Lynch, K. A., and Holtet, J. A., "The cleft ion plasma environment at low solar activity," , Vol. 23, No. 14, 1996, pp. 1877–1880. https://doi.org/10.1029/96GL00843.

[72] McAdams, K. L., LaBelle, J., Schuck, P. W., and Kintner, P. M., "PHAZE II observations of lower hybrid burst structures occurring on density gradients," , Vol. 25, No. 16, 1998, pp. 3091–3094. https://doi.org/10.1029/98GL02424.

[73] Meyer-Vernet, N., Hoang, S., Issautier, K., Maksimovic, M., Manning, R., Moncuquet, M., and Stone, R. G., "Measuring Plasma Parameters With Thermal Noise Spectroscopy," *Geophysical Monograph Series*, Vol. 103, 1998, p. 205. https://doi.org/10.1029/GM103p0205.

[74] Jensen, M. D., and Baker, K. D., "Measuring Ionospheric Electron Density Using the Plasma Frequency Probe," *Journal of Spacecraft and Rockets*, Vol. 29, No. 1, 1992, pp. 91–95. https://doi.org/10.2514/3.26318.